

# Design and Fabrication of Multi-microelectrode Array for Neural Prosthesis

Ming-Shaung Ju\* Hsin-Chun Chien Gin-Shin Chen Chou-Ching K. Lin<sup>1</sup>  
Cheng-Hung Chang<sup>2</sup> Chi-Wen Chang<sup>3</sup>

*Department of Mechanical Engineering, National Cheng Kung University, Tainan, Taiwan, 701 ROC*

<sup>1</sup>*Department of Neurology, University Hospital, National Cheng Kung University, Tainan, Taiwan, 701 ROC*

<sup>2</sup>*Department of Biomedical Engineering, National Cheng Kung University, Tainan, Taiwan, 701 ROC*

<sup>3</sup>*Department of Neurosurgery, University Hospital, National Cheng Kung University, Tainan, Taiwan, 701 ROC*

Received 8 October 2001; Accepted 8 April 2002

---

## Abstract

A multi-microelectrode system for neuroprostheses was designed and manufactured by using microfabrication technologies. For biocompatibility, we used silicone rubber as the base layer, polyimide as the insulation layer and gold as the conduction material. A model simulating the electric properties of the microelectrode array was developed for system design. The electrode system was planar and consisted of 18 microelectrodes. The contact area of each microelectrode was 600 x 400  $\mu\text{m}$ . The sensing capability of the microelectrode system was tested in animal experiments. We put the system underneath the sciatic nerve of New Zealand rabbit and passively move the ankle joint. The results showed that the system could record changes in neural signals during movements. Analyses of the recorded signals and the joint angle revealed that the recorded neural signals had good correlation with the weighted sum of joint angle and angle velocity. In conclusion, we developed a planar multi-microelectrode system, which could sense neural signals in acute animal experiments.

**Keywords:** Neural prosthesis, Microelectrode, Electroneurography

---

## Introduction

Neural prosthesis, a new and growing development in rehabilitation, takes the advantage of intact peripheral nerves to improve the motor functions of patients with lesions in central nervous system. The advantages include less electrical current for stimulation (as compared with intramuscular and epimesial electrodes), less wiring for communication between parts and no need for designing artificial sensors. On the other hand, the extra costs include larger risk of nerve injury, more calculation load to recognize the acquired signals and more effort to manufacture the prosthetic system. To develop a neural prosthesis may involve many technologies, such as tissue engineering, RF telemetry and micro-electrico-mechanical system (MEMS) technology. In particular, fabrication of microelectrode system plays the central role. Ideally, the system should be easy to fabricate, small in size, reliable, biocompatible, harmless to the nerve fibers and multi-polar.

Many microelectrode systems were proposed for different purposes [1-5], which could be roughly divided into two categories according the placement of electrode inside or outside the nerve fascicles, i.e., extrafascicular and intrafascicular. The advantage of intrafascicular electrode is much larger amplitude of signals, as seen in conventional microneurography [6]. Yet, for long-term usage, the intrafascicular penetration may cause injury to nerve itself and may not be easily fixed at the desired position. When the dimension of microelectrode system increases as the number of microelectrodes increases, the problem becomes more serious. On the other hand, the advantages of extrafascicular placement include less invasive procedures and easy fixation. Yet, the very small amplitude of signal and low signal/noise ratio have to be dealt with and there is a risk of encroachment of the nerve if cuff type configuration is used.

The goal of this study is to develop a planar extrafascicular multi-microelectrode system, which is small, stable, selective and minimally invasive. The electrode itself may not be suitable for long-term fixation. Yet, this is the first step toward chronic implantation. The challenges are mainly twofold: (1) how to manufacture the electrode system

---

\* Corresponding author: Ming-Shaung Ju  
Tel: +886-6-2757575 ext.62163; Fax: +886-6-2352973  
E-mail: msju@mail.ncku.edu.tw

using biocompatible materials and (2) how to confirm the usability of the electrode, i.e., the electrode system can capture the neural signals.

**Methods**

**Design of microelectrodes**

The major considerations in microelectrode design were material properties and electrical characteristics. For the material properties, the component materials should be all biocompatible and biologically stable. We chose the medical grade silicone rubber sheet as the base, polyimide (PI) for insulation layer and gold for conduction material. For the electrical characteristics, the bandwidth of the electrode system should cover the bandwidth of the neural signals in the peripheral nerves (500-5000 Hz) [7]. To assist designing we developed an equivalent electric circuit model, which consisted of solution-electrode interface model, the conducting part and the interaction between conducting parts (Figure 1). The interfacial interaction was modeled as a parallel resistance (Rt) and capacitance (Ci) in series with a spreading resistance (Rs) [8],

$$R_i = \frac{R \cdot T}{J_0 \cdot z \cdot F} \tag{1}$$

$$C_i = \frac{1}{C_H} + \frac{1}{C_D} \tag{2}$$

$$R_s = \frac{r_L \cdot \ln\left(\frac{4 \cdot L}{W}\right)}{p \cdot L} \tag{3}$$

where R was Boltzman gas constant, z was the valence of ions, T was the absolute temperature, F was Faraday constant, J0 was the current density, L was the conductivity (Ome\*cm) of the solution, L and W was the length and width of the electrode, CH was Helmholtz capacitance and CD was the Gouy-Chapman capacitance. The electrode (Re1), connecting wire (Re2) and bonding pad (Re3) were modeled as pure resistances,

$$R_{e_i} = \frac{\rho \cdot t}{A_i} \quad i = 1, 2, 3 \tag{4}$$

where  $\rho$  was the resistivity, t was the thickness and A1, A2 and A3 were the areas of the electrode contact part, conducting wire and bonding pad, respectively. The interaction between conducting parts was described as pure capacitances CS (between electrodes and between bonding pads) and CC (between conducting wires),

$$C_c = 2\epsilon_0 \cdot \epsilon_r \cdot L \cdot \left[ 0.03 \left( \frac{W}{H} \right) + 0.83 \left( \frac{t}{H} \right) - 0.07 \left( \frac{t}{H} \right)^{0.222} \right] \cdot \left( \frac{S}{H} \right)^{-1.34} \tag{5}$$

$$C_s = \frac{1.15\epsilon_0 \cdot \epsilon_r \cdot L \cdot W}{H} + 2.8\epsilon_0 \cdot \epsilon_r \cdot L \cdot \left( \frac{t}{H} \right)^{0.222} \tag{6}$$

where W was the width of conducting part, H was the thickness of insulation layer, S was the distance between conducting parts,  $\epsilon_0$  was the dielectric permittivity of free space and  $\epsilon_r$  was the relative dielectric permittivity of the medium between the two conductors. The values of constants Re i, CC, Rt, Ci, CS and RS were taken or calculated from the experimental data in the literature [9]. The model was simulated by using Matlab with Simulink (www.mathworks.com). The frequency response of the system was obtained by changing the input frequency sequentially. The values of four design parameters (W, S, H, A1) were changed systematically to see the effects of each parameter. Figure 2(a) was a photograph of the final prototype and Figure 2(b) showed both the top and the cross-sectional views of the microelectrode system.

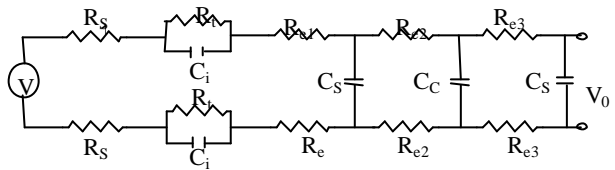
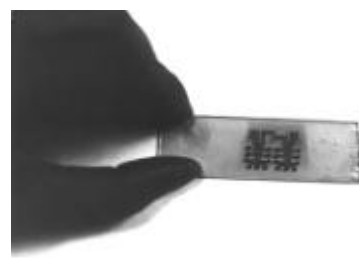
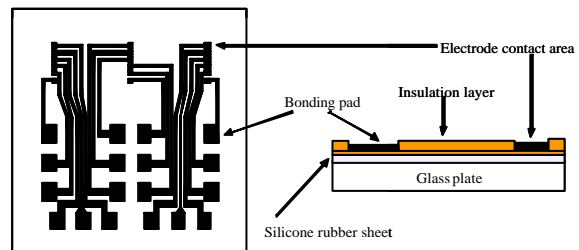


Figure 1. The equivalent model of the microelectrode circuit. V was the input source and V0 was the measured signal.



(a)



(b)

Figure 2. The layout of the multi-microelectrode system. (a) was a photograph of the final prototype, (b) schematically

showed the top view on the left and the cross-sectional view on the right.

### Fabrication

As far as the authors knew, no papers in the literature formally described the fabrication process of micro-electrical circuits on the silicone rubber sheet. The metal pads in the classical cuff electrode were accomplished manually [10]. So we had to develop the fabrication process by try and error. First, we lay a thin silicone rubber sheet (1.25 mm) on a glass plate for the convenience of processing. A layer of PI (~10 μm) was spin coated onto the silicone rubber sheet as the insulation layer. Second, metal gold was evaporated to form the conducting layer (~0.5 μm) on top of the PI layer and photo-etched by the standard photolithography with the first mask to create 18 microelectrodes. The size of each electrode contact area was 600 x 400 μm<sup>2</sup>. Third, another PI layer (6 μm) was spin-coated onto the metal layer and photo-etched with the second mask to expose the electrode contact areas and the bonding pads. The wires to the amplifiers were soldered to the bonding pads manually under a dissecting microscope.

### Experimental procedure

The experimental apparatus consisted of a high gain and high impedance amplifier and a computer equipped with an analog-digital conversion board. We used New Zealand white male rabbits (2-2.5 kg) as the experimental subjects. Animals were anesthetized with Ketamine injected intramuscularly and the skin area to be operated was prepared with the standard aseptic procedure. The incision was made on the lateral side of the thigh to expose a segment of sciatic nerve before the nerve bifurcated into peroneal and tibial nerves. The sciatic nerve was carefully not too extensively dissected and lifted off slightly out the underlying fascia plan. Then, the custom-designed multi-microelectrode system was inserted beneath the nerve. The nerve and the microelectrode system together were covered with a thin layer of inert oil. The animal together with the pre-amplifier was placed in a custom-made copper-web cage to prevent the interference of surrounding electromagnetic waves. The signal received by the electrode, i.e., electroneurography (ENG), was amplified 105 times and filtered with a hardware band-pass filter (500-5000 Hz). In addition to the custom-made microelectrode system, we inserted a standard concentric needle electrode to the muscle beneath the microelectrode system to record electromyography (EMG) for comparison and analyses. The EMG signal was amplified 5000 times and filtered with a hardware band-pass filter (100-5000 Hz).

We elicited sensory signals by manually changing the ipsilateral ankle joint angle. We tried to do the movement consistently, either in dorsiflexion or plantar flexion direction. Each movement lasted about 5 seconds and separated with enough time for preventing the effects of previous movements. The angle trajectory was recorded by a variable-resistance electrogoniometer with a four-parallel bar mechanism [11]. All the signals (ENG, EMG and joint angle) were digitized at 20K Hz per channel and stored in the computer for off-line analyses.

For the control study, we applied jelly-form Xylocaine, a local anesthetic, to the sciatic nerve distal to the segment of

Table 1. Results of the simulation.

Case	Parameters (m)				Bandwidth (Hz)
	W	S	H	Ap	
1	200	400	10	400 x 600	1.81 M
2	200	20	5	70 x 70	10 K
3	500	20	5	140 x 140	10 K

electrode application and repeated ankle movements at 2.5, 4 and 8 minutes after the application of the anesthetic.

### Signal analysis

The stored signals were transformed to the frequency domain by Fourier transformation for analyzing the changes in frequency content. Also, the signals were smoothed with moving average, i.e., calculating root mean squares (RMS) of 200 points and moving without overlap for evaluating the correlation between channels.

We also developed a simple model for fitting the recorded ENG. We assumed that ENG signal was proportional to the weighted sum of angular position ( $x$ ) and angular velocity ( $\dot{x}$ ),

$$y = ax + b\dot{x} + c \quad (7)$$

where  $a$ ,  $b$  and  $c$  were constant parameters to be estimated. For estimating parameters ( $a$ ,  $b$  and  $c$ ), since the model was linear, we first derived analytic solution of minimum with the cost function defined as the least squared errors and calculated the parameters accordingly.

## Results

### Simulation of the electrode

The results of simulating the microelectrode circuit model were shown in Table 1. The effect of changing  $S$  was relatively small. Case 1 was the dimension of current planar microelectrode system and its bandwidth was 1.81M (Hz), which was obviously higher than the demand of the neural bandwidth. Alternatively, if we set 10K Hz as the lower limit of the highest passband frequency and changed the design parameters to see the allowable ranges of parameters. Table 1 showed two possible limit dimensions of the microelectrode system. The limit dimension was well smaller than the currently designed multi-microelectrode system. The results indicated that we could design a new system with more packed smaller microelectrodes.

### Neural Recording

The results of extending (plantar flexion) the animal ankle were shown in Figure 3. Figure 3(a) showed the angle

trajectory. The magnitude of ENG (Figure 3(c)) changed with the angle trajectory, while EMG (Figure 3(b)) showed no similar trend. RMS of ENG (Figure 3(d)) showed the

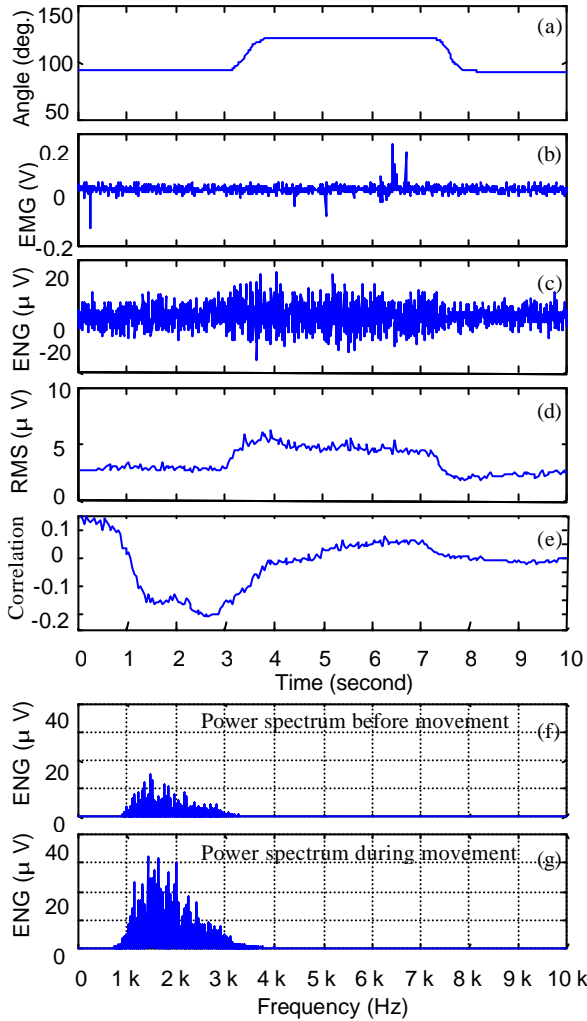


Figure3. The response of the microelectrode system during plantar flexion. (a) joint angle trajectory, (b) EMG, (c) ENG, (d) RMS of ENG, (e) correlation between EMG and ENG, (f) and (g) power spectrum of ENG in one second interval (first and sixth second) at two different angles.

changes in ENG more clearly and definitely. The correlation between ENG and EMG signals (Figure 3(e)) was low, which eliminated the possibility that ENG signal was a contaminating artifact of EMG signal. Figures 3(f) and 3(g) showed the power spectrums of ENG before and during the movement. The power in the passband increased during the joint movement. Similar shapes of the power spectrum before and during the movements reflected the passband of the hardware filter.

The results of dorsiflexing the ankle joint were shown in Figure 4. ENG decreased with dorsiflexion. Again, the correlation between ENG and EMG was minimal. The power in the passband decreased during the joint movement.

The results of the multi-channel recording were shown in Figure 5, in which E1, E2 and E3 were ENG signals from different electrodes of the same multi-microelectrode system. The magnitudes of signals in E1 and E2 were clearer and had similar trend, while E3 signal was not. From Figure 5(h), the

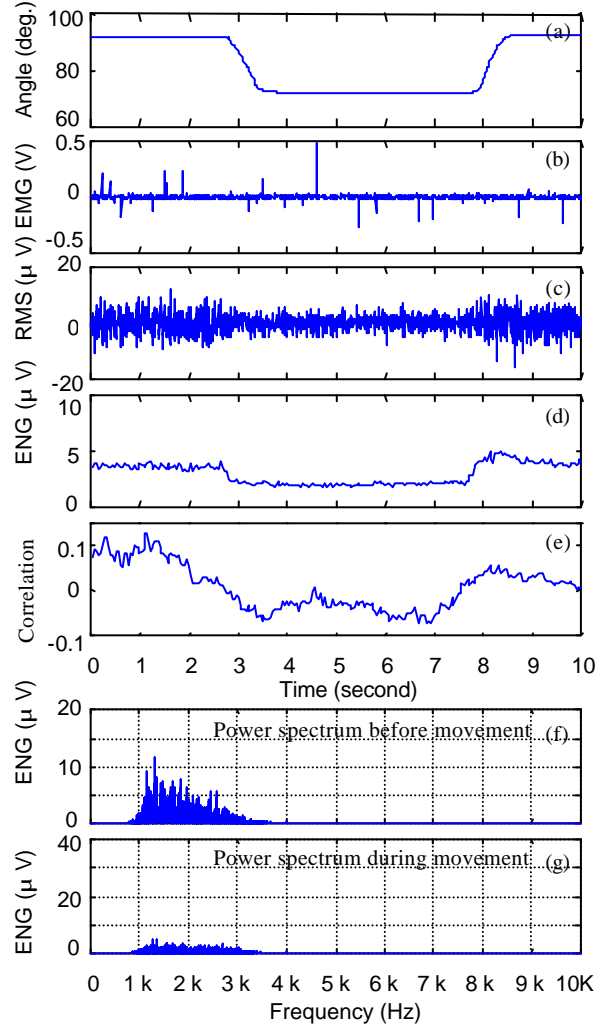


Figure 4. The response of the microelectrode system during dorsiflexion. The convention was identical as in Figure 5.

correlation between E1 and E2 signals was higher because E1 and E2 electrodes were closer and in good contact with the nerve. The correlation between E1 and E3 signals was lower. During the experiment, we observed that the E3 electrode was on the lateral edge of nerve.

**Control studies**

The results of control study were shown in Figure 6. After applying Xylocaine, while the magnitude of background activity decreased slightly, the magnitude of movement related changes decreased more markedly with time gradually. After eight minutes, moving ankle joint

produced only mild change in ENG amplitude. The blocking effects lasted about 30 minutes. The results indicated that the blocking effects actually came from Xylocaine, since it took time for Xylocaine to diffuse into nerve fibers. Also, the

changes in ENG were really sensory signals conducted via the nerve fibers, not the motion artifact transmitted through connective or muscle tissues.

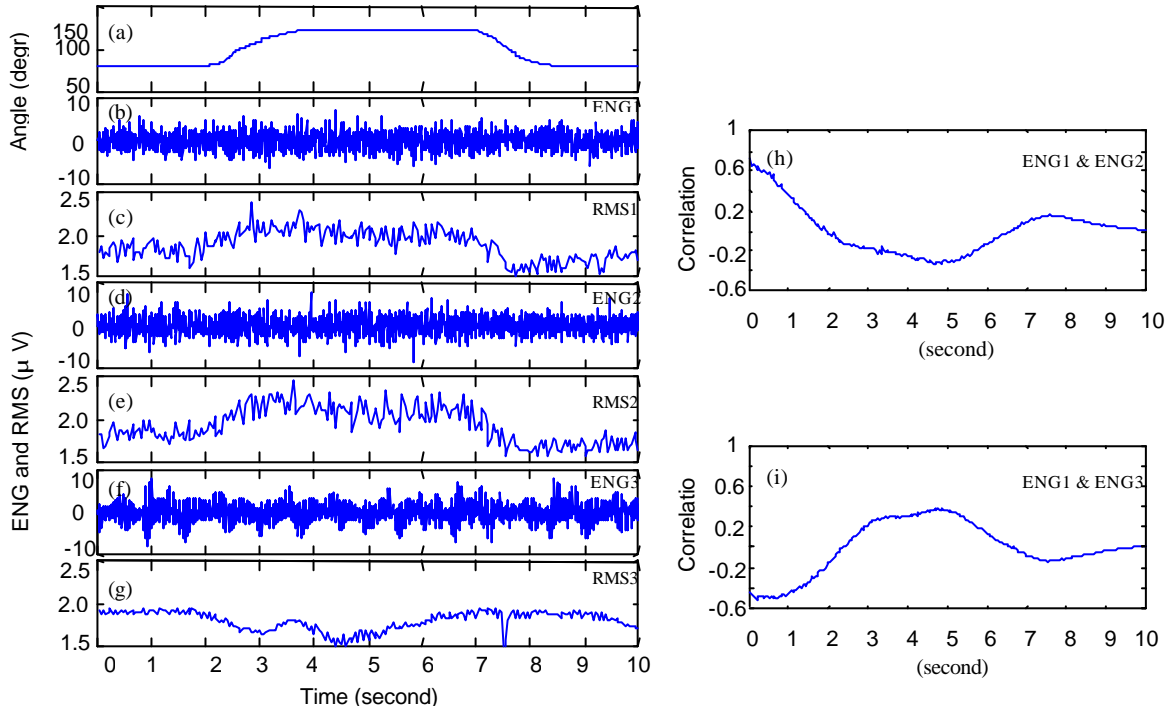


Figure 5. The responses of three microelectrodes in the same microelectrode system during plantar flexion.

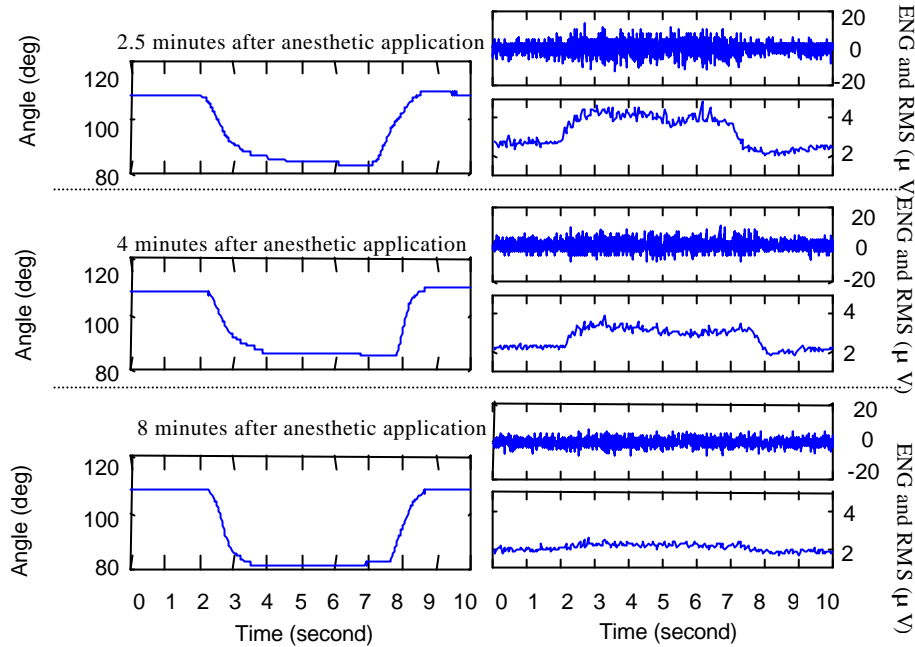


Figure 6. The influence of Xylocaine on the ENG signal. The upper, middle and lower sets of plots represented ENG response to passive joint movements 2.5, 4 and 8 minutes after the application of Xylocaine, respectively.

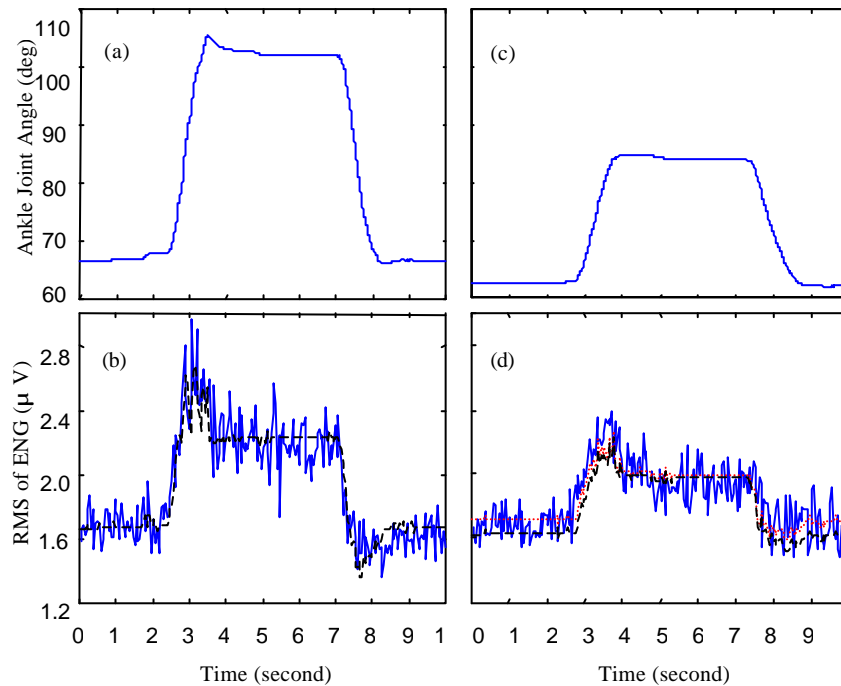


Figure 7. The model results of ENG signals as a function of knee joint angles. In (b) and (d), the solid lines were the experimental ENG RMS corresponding to joint movements (a) and (c) and the dashed lines were the simulated results using parameters derived from 40 degrees movement. The dotted line in (d) was the simulated results using parameters derived from 20 degrees movement.

### Model results

Figure 7 showed the simulation results with the ENG model. We did similar ankle joint movements. We first estimated the parameters of the model with 40 degrees plantar flexion ( $a = 0.009$ ,  $b = 0.016$  and  $c = 0.613$ ) and then simulated ENG signal. The simulated trajectory fitted the experimental data well. When we used the parameters derived from the 40 degrees movement to simulate the results of 20 degrees plantar flexion, the simulated trajectory also fitted the experimental data well, except a relatively constant bias. We estimated the parameters again with 20 degrees movement data ( $a = 0.009$ ,  $b = 0.013$  and  $c = 0.874$ ). The derived parameters fitted better. When we compared two sets of parameters, we found that the main difference was the constant term ( $c$ ). This result indicated that ENG signal could be predicted well with a function consisting linearly weighted summation of joint angle and angular velocity. The uncertain term was the variable background level.

## Discussion

### Electrode dimension

We chose the dimension of the microelectrode based on the dimension of the animal sciatic nerve and the results of circuit model simulation. There was dilemma between the choices of larger or smaller electrode size. Larger electrode had the advantage of collecting signals from large number of

nerve fibers. On the other hand, smaller electrode had the advantage of high impedance and larger signal amplitude, at the cost of larger noise level. Our current circuit model did not take these factors into consideration. We are working on improving the model.

### Movement artifacts

In current study, we moved the ipsilateral ankle joint to observe the change in ENG magnitude. This procedure introduced several potential sources of artifacts. First was the movement artifact, which was transmitted through the connective tissues. Second was the change of potential field, as the human body was also a conductor. Third was the direct traction of the nerve. Fourth was the cutaneous touch and pressure sensory inputs. We performed a control study to rule out these possibilities. The results of control study excluded all above-mentioned possibilities, except the direct traction of the distal part of the nerve distal to the blocking point. It was difficult to prove the source of ENG magnitude change was on the sensory organ generator or the distal part of the nerve. The problem was even more complicated when we recalled that the signal source of some nerve endings was the deformation of the end part of the nerve fiber. Since in the normal movements, either active or passive, would also tract the nerve, we thought it was not important to distinguish whether the generator site was the sensory organ or the distal endings of the nerve fibers. It was clear that the surgical procedure, which freed the nerve out of the connective tissue,

did not cause movement artifacts between the nerve and the microelectrode system.

### Model results

The preliminary results of ENG model showed that the simulated results matched the experimental results well. Yet, there remained several problems if ENG was to be used to predict the joint angle. First was that we did the experiment only in a small range of movements (20 to 40 degrees). There were reports that ENG might not faithfully reflect joint angle at both extreme ends [12]. Second, the threshold, which represented the background noise level, also represented the lower limit of detectable angle range. The solution to this problem would be a better amplifier with lower background noise level. Third, the variable background level might be a reflection of other neglected sensory information. It could not be easily solved unless more understanding of other sensory sources.

### Contents of ENG

We did experiments on several animals and found that the direction of ENG amplitude change and joint angle change was not constant, i.e., dorsiflexion of ankle joints increased ENG magnitude in some animal subjects and decreased in others. Theoretically, moving the joint in either direction stretched muscles on one side and shortened muscles on the other sides. The discharge rate of afferents from muscle spindles in the stretched muscle would increase and vice versa. So, it was difficult to predict ENG amplitude would increase or decrease with dorsiflexion. We suspected that the direction of change might be different, depending on the recording site along the perimeter of the nerve trunk. This would explain why sometimes ENG amplitude increased and sometimes decreased with dorsiflexion in different animals with the same settings. In order to solve this problem, more densely packed microelectrode system in the future would be required.

Though we found that the changes in ENG correlated well with angle and angular velocity, we did not assert that ENG only contained these channels of information. At our experimental setting, the magnitudes of motor efferent and the force afferent were relatively small. We also neglected the exteroceptive information, such as cutaneous pain, temperature and touch sensations. It would be a big and interesting challenge to separate these channels of information.

Currently, we are working on refining the multi-microelectrode system in two directions. One is to design

smaller and more densely packed system and the other is to convert the planar configuration into cuff one.

### Conclusions

We successfully developed a planar multi-microelectrode system. The system could detect changes in ankle joint angle. The information contained in ENG was found to be a combination of angle and angular velocity.

### Acknowledgement

This work is partly supported by a grant, NHRI-EX90-9017EP, from National Health Research Institute, Taiwan.

### References

- [1] M. Kuperstein and D. A. Whittington, "A practical 24 channel microelectrode for neural recording in vivo", *IEEE Trans. BME*, 28: 288-293, 1981.
- [2] D. J. Edell, "A peripheral nerve information transducer for amputees: long-term multichannel recordings from rabbit peripheral nerves", *IEEE Trans. BME*, 33: 203-214, 1986.
- [3] J. Rozman, "Multielectrode cuff for extraneural selective stimulation of nerve fibers", *J. Med. Eng. Technol.*, 16: 194-203, 1992
- [4] J. J. Struijk, M. Thomsen, J. O. Larsen and T. Sinkjær, "Cuff electrodes for long-term recording of natural sensory information", *IEEE Eng. Med. & Biol. Mag.*, 18: 91-8, 1999.
- [5] C. Gonzalez, and M. Rodriguez, "A flexible perforated microelectrode array probe for action potential recording in nerve and muscle tissues", *J. Neurosci. Methods*, 72: 189-195, 1997.
- [6] K. Hagbarth, "Microneurography and applications to issues of motor control: fifth annual Stuart Reiner memorial lecture", *Muscle Nerve*, 16: 693-705, 1993.
- [7] A. Boulton, B. Baker and H. Vanderwolf, *Neurophysiological Techniques Applications to Neural systems*, Clifton, NJ: Human Press, 65-91, 1990.
- [8] G. T. A. Kovacs, Technology development for a chronic neural interface, Ph.D. Dissertation, Stanford University, CA, USA, 1990.
- [9] T. Sakurai and K. Tamaru, "Simple formulas for two- and three-dimensional capacitances", *IEEE Trans. Electron. Devic.*, 30: 183-185, 1983.
- [10] G. G. Naples, J. T. Mortimer, A. Scheiner and J. D. Sweeney, "A spiral nerve cuff electrode for peripheral nerve stimulation", *IEEE Trans. BME*, 35: 905-915, 1988.
- [11] D. A. Winter, *Biomechanics of Human Movement*, New York: John Wiley & Sons, 12-14, 1979.
- [12] W. Jensen, R. Riso, F. Sepulveda and T. Sinkjær, "Angular resolution and working ranges of flexion-extension information in nerve cuff recordings of muscle afferent activity", *Proc. 6<sup>th</sup> Ann. Conf. IFESS*, 205-207, 2001.